

Zonal Flow as Pattern Formation: Merging Jets and the Ultimate Jet Length Scale

Jeffrey B. Parker* and John A. Krommes†

Princeton University, Princeton Plasma Physics Laboratory, Princeton, New Jersey 08543, USA

(Dated: June 11, 2022)

Zonal flows are well known to arise spontaneously out of turbulence. It is shown that for statistically averaged equations of quasigeostrophic turbulence on a beta plane, zonal flows and inhomogeneous turbulence fit into the framework of pattern formation. There are many implications. First, the zonal flow wavelength is not unique. Indeed, in an idealized, infinite system, any wavelength within a certain continuous band corresponds to a solution. Second, of these wavelengths, only those within a smaller subband are linearly stable. Unstable wavelengths must evolve to reach a stable wavelength; this process manifests as merging jets.

Introduction Zonal flows — azimuthally symmetric, generally banded, shear flows — are spontaneously generated from turbulence and have been reported in atmospheric [1], oceanic [2], and laboratory plasma [3] contexts. Recently, they have also been observed in astrophysical simulations [4]. In magnetically confined plasmas, zonal flows are thought to play a crucial role in regulation of turbulence and turbulent transport [5].

Zonal flows remain incompletely understood, even regarding the basic question of the jet width. Various authors have attempted to relate the jet width or spacing to length scales that emerge from the vorticity equation by heuristically balancing the magnitudes of the Rossby wave term and the nonlinear advection term. Those scales include the Rhines scale $(U/\beta)^{1/2}$, where U is the rms velocity and β is (in planetary contexts) the northward gradient of the Coriolis parameter [6], and a related transitional scale obtained by using the energy input ε rather than U [7]. It is often asserted that an inverse energy cascade is arrested at one or another of those scales by the generation of Rossby waves, which then preferentially sends energy into zonally elongated structures. However, others have concluded that the inverse cascade cannot be stopped by a β effect but only by friction [1, 8]. Furthermore, it has been suggested that the primary mechanism maintaining the jets is instead a spectrally nonlocal interaction with turbulence at small scales [9]. Regardless of the physical mechanism involved, heuristic balances are not systematically derived or quantitatively predictive.

A related topic is the merging of jets. Coalescence of two or more jets is ubiquitous in numerical simulations [9–11]. The merging process occurs during the initial transient period before a statistically steady state is reached. It is clear that the merging is part of a dynamical process through which the zonal flow reaches its preferred length scale, but there has been little theoretical understanding of the merging phenomenon. Insights into jet structure are valuable for explaining various features of weather and for untangling a host of nonlinear processes in plasmas, including details of transitions between modes of low and high confinement.

Our present work addresses these questions in the con-

text of stochastically forced quasigeostrophic (QG) flow on a β plane, a model for fluid turbulence in a rotating system [7]. It is known that the QG equation for potential vorticity is nearly mathematically identical to the generalized Hasegawa–Mima equation [12, 13] for electrostatic potential, a model for magnetized plasma turbulence in the presence of a background density gradient. Importantly, numerical simulations of both models can display emergence of steady zonal flows. We concentrate on the QG model because it has been studied far more extensively in the literature. However, our methodology is equally applicable to the Hasegawa–Mima equation, as we will describe in a future, more detailed article.

We study a statistical average of the QG equation. Statistical approaches enable one to gain physical insight by averaging away the details of the turbulent fluctuations and working with smoothly varying quantities. Sometimes, statistical turbulence theories strive for quantitative accuracy, which requires rather complicated methods [14]. In contrast, our investigation is at a more basic level and concerns the fundamental nature of zonal flows interacting self-consistently with inhomogeneous turbulence.

We discover that the statistically averaged system possesses the mathematical structure of pattern formation. Pattern formation is the study of systems out of thermal equilibrium that spontaneously generate spatial patterns [15–20]. Application of its theory to the averaged system leads to insights that are difficult to discern by studying one realization of the turbulence.

Two important results follow that are general properties of pattern formation systems. First, the zonal flow wavelength is not unique. Indeed, in an idealized, infinite system, any wavelength within a certain continuous band corresponds to a steady-state solution. Second, of these wavelengths, only those within a smaller subband are linearly stable. Unstable wavelengths must evolve to reach a stable wavelength. For short (long) wavelength unstable jets, this process manifests as merging (branching) jets.

Quasigeostrophic equation and CE2 model Our basic model is two-dimensional quasigeostrophic turbulence on

a β plane in the limit of infinite deformation radius,

$$\partial_t w + \mathbf{v} \cdot \nabla w + \beta \partial_x \phi = \xi - \mu w - \nu(-1)^h \nabla^{2h} w, \quad (1)$$

where w is the relative vorticity, ϕ is the streamfunction such that $w = \nabla^2 \phi$, $\mathbf{v} = \hat{\mathbf{z}} \times \nabla \phi$ is the horizontal fluid velocity, $\hat{\mathbf{z}}$ is in the vertical direction, μ is the constant friction, ν is the viscosity with hyperviscosity factor h , and ξ is small-scale white-noise forcing. The zonal flow behavior in numerical simulations of Eq. (1) is shown in Fig. 1(a). During the transient period, merging jets are observed, while in the late time, a statistically steady state is reached with stable unwavering jets.

We restrict ourselves to the quasilinear (QL) approximation of this system. To obtain the QL equations, we perform an eddy-mean decomposition, given by decomposing all fields into a zonal mean and a deviation from the zonal mean, then neglect the eddy-eddy nonlinearities within the eddy equation [11]. The QL model exhibits the same basic zonal jet features as the full model, namely merging jets and the formation of stable jets.

We consider a statistical average of the QL system. In the presence of steady zonal flows, a statistical homogeneity assumption is clearly invalid. Therefore, we allow the turbulence to be inhomogeneous in the direction of zonal flow variation (y). The averaged equations, referred to as the second-order cumulant expansion (CE2), are [11]

$$\begin{aligned} \partial_t W + (U_1 - U_2) \partial_x W - (U_1'' - U_2'') \left(\nabla^2 + \frac{1}{4} \partial_{\bar{y}}^2 \right) \partial_x C \\ - [2\beta - (U_1'' + U_2'')] \partial_{\bar{y}} \partial_y \partial_x C \\ = F - 2\mu W - 2\nu D_h W, \end{aligned} \quad (2a)$$

$$\partial_t U + \partial_{\bar{y}} \partial_y \partial_x C(0, 0, \bar{y}, t) = -\mu U - \nu(-1)^h \partial_{\bar{y}}^{2h} U, \quad (2b)$$

where x and y represent two-point separations, \bar{y} represents the two-point average position (if the turbulence were homogeneous, there would be no \bar{y} dependence), $W(x, y | \bar{y}, t)$ and $C(x, y | \bar{y}, t)$ are the one-time, two-space-point correlation functions of vorticity and streamfunction, $U(\bar{y}, t)$ is the zonal flow velocity, $U_1 = U(\bar{y} + y/2, t)$, $U_2 = U(\bar{y} - y/2, t)$, $F(x, y)$ is chosen to be isotropic, homogeneous ring forcing as in [11], and D_h is the hyperviscosity operator. The relation between W and C can be found in [11].

Given the assumption that the stochastic forcing ξ is white (delta-correlated) noise, the only further assumptions necessary for CE2 to be an exact description of the QL model are statistical homogeneity and ergodicity in the zonal (x) direction. This is because the QL model neglects the nonlinear eddy-eddy term that would give rise to a closure problem. Alternatively, CE2 can be regarded as a drastically truncated statistical closure of the full QG model [21–24]. However, for present purposes we prefer the former interpretation.

The CE2 equations exhibit several important symme-

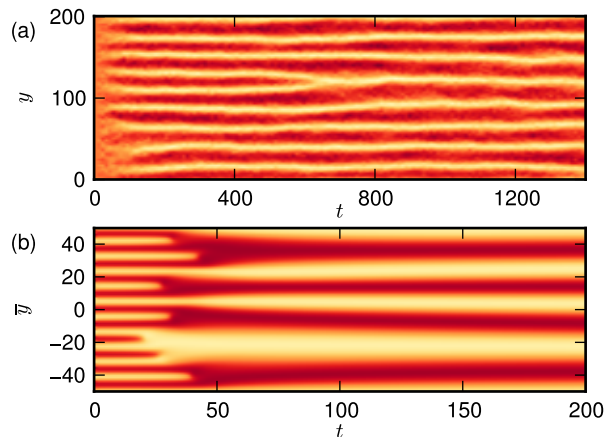


FIG. 1. (a) Merging jets during the transient regime of the QG equation (1) (zonal-mean velocity is shown). (b) Merging behavior observed in the amplitude equation (4) [$\text{Re } A(\bar{y}, t)$ is shown].

tries of translation and reflection, given by

$$\bar{y} \rightarrow \bar{y} + \delta \bar{y}, \quad (3a)$$

$$x, \bar{y} \rightarrow -x, -\bar{y}, \quad (3b)$$

$$y, \bar{y} \rightarrow -y, -\bar{y}, \quad (3c)$$

$$x, y \rightarrow -x, -y. \quad (3d)$$

CE2 has been studied extensively numerically [21–24]. Those simulations also exhibit merging jets [22].

Zonostrophic Instability and the Amplitude Equation For Eq. (2) there always exists a homogeneous equilibrium, which arises from a simple balance between forcing and dissipation: $W = (2\mu + 2\nu D_h)^{-1} F$, $U = 0$. This equilibrium is stable in a certain regime of parameters. As a control parameter such as the friction μ is varied, this homogeneous state becomes zonostrophically unstable [11, 22]. Physically, zonostrophic instability occurs when dissipation is overcome by the mutually reinforcing processes of eddy tilting by zonal flows and production of Reynolds stress forces by tilted eddies. The instability eigenmode consists of perturbations spatially periodic in \bar{y} with zero real frequency [11], so that zonostrophic instability arises as a Type I_s instability [15] of homogeneous turbulence.

Just beyond the instability threshold, a bifurcation analysis yields a perturbative amplitude equation for the bifurcating mode. This amplitude equation is constrained by the translation and reflection symmetries (3) to take a universal form [15]. The amplitude equation, sometimes referred to as the real Ginzburg-Landau equation, is

$$\partial_t A(\bar{y}, t) = A + \partial_{\bar{y}}^2 A - |A|^2 A, \quad (4)$$

where all coefficients have been rescaled to unity. Here, A is the complex, spatially varying amplitude of the eigenvector that is neutrally stable at the bifurcation point.

The minus sign in the last term corresponds to a supercritical bifurcation, which has been demonstrated numerically to occur [22].

The amplitude equation (4) is well understood [15–17], and much of its qualitative behavior is seen generically in pattern formation systems. First, a steady-state solution exists for any wave number within the continuous band $-1 < k < 1$ (to see this, observe that $A = \alpha e^{ik\bar{y}}$ with $|\alpha|^2 = 1 - k^2$ is a solution). Second, only solutions with $k^2 < 1/3$ are stable [16]. This is demonstrated in Fig. 1(b), where an unstable solution that has been slightly perturbed undergoes merging behavior until a stable wave number is reached.

These qualitative behaviors are also exhibited by the CE2 system. In the following sections we calculate the equilibria and stability of CE2.

Calculation of Ideal States We proceed to find the steady-state solutions of Eq. (2). In the context of an infinite domain with no boundaries, these solutions are referred to as ideal states. Let q denote the basic zonal flow wave number of an ideal state. For a given q , we solve the time-independent form of Eq. (2) directly. This approach is distinct from time integration of Eq. (2) to a steady state, which is done in [21–24] within a finite spatial domain. Our procedure has two advantages, both related to the fact that ideal states exist for any q within a continuous band. First, we can specify precisely the q of the desired solution. Second, we can solve directly for all solutions, including unstable ones, rather than find only those which develop from time evolution.

An ideal state is represented as a Fourier-Galerkin series with coefficients to be determined [16, 19, 20]. We expand as follows:

$$U(\bar{y}) = \sum_{p=-P}^P U_p e^{ipq\bar{y}}, \quad (5a)$$

$$W(x, y | \bar{y}) = \sum_{m=-M}^M \sum_{n=-N}^N \sum_{p=-P}^P W_{mnp} e^{imax} e^{inby} e^{ipq\bar{y}}. \quad (5b)$$

While the periodicity in \bar{y} is desired, the correlation function should decay in x and y ; periodicity in x and y is a consequence of using the convenient Fourier basis. Thus, a and b , unlike q , are numerical parameters. They represent the spectral resolution of the correlation function and should be small enough to obtain an accurate solution.

The CE2 symmetries allow us to seek a solution where $U(\bar{y}) = U(-\bar{y})$ and $W(x, y | \bar{y}) = W(-x, -y | \bar{y}) = W(x, -y | -\bar{y}) = W(-x, y | -\bar{y})$. These constraints, along with reality conditions, force U_p to be real, $U_p = U_{-p}$, and $W_{mnp} = W_{-m,n,p}^* = W_{m,-n,p}^* = W_{m,n,-p}^*$.

We obtain a system of nonlinear algebraic equations for the coefficients U_p, W_{mnp} by substituting the Galerkin

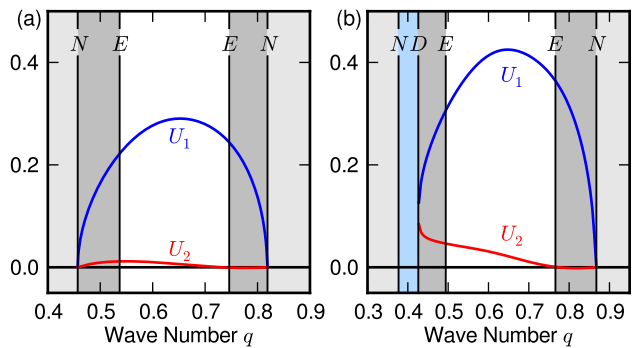


FIG. 2. Zonal flow amplitude U_1, U_2 as a function of ideal state wave number q at (a) $\mu = 0.21$ and (b) $\mu = 0.19$. In the unshaded region, ideal states are stable. The vertical lines correspond to various instabilities which separate the regions (see Fig. 3).

series into Eq. (2) and projecting onto the basis functions. To demonstrate the projection for Eq. (2a), let $\phi_{mnp} = e^{imax} e^{inby} e^{ipq\bar{y}}$. We project Eq. (2a) onto ϕ_{rst} by operating with

$$\left(\frac{2\pi}{a} \frac{2\pi}{b} \frac{2\pi}{q} \right)^{-1} \int_{-\pi/a}^{\pi/a} dx \int_{-\pi/b}^{\pi/b} dy \int_{-\pi/q}^{\pi/q} d\bar{y} \phi_{rst}^*. \quad (6)$$

For instance, the term $(U_1 - U_2)\partial_x W$ projects to $I_{rstp'mnp}^{(1)} U_p W_{mnp}$, where repeated indices are summed over, $I_{rstp'mnp}^{(1)} = ima(\sigma_1 - \sigma_2)\delta_{m,r}\delta_{p'+p-t}$, $\sigma_{1,2} = \text{sinc}(\alpha_{1,2}\pi/b)$, and $\alpha_{1,2} = nb - sb \pm p'q/2$. The other terms of Eq. (2a), as well as Eq. (2b), are handled similarly. In total, we generate as many equations as there are coefficients.

The system of nonlinear algebraic equations is solved with a Newton's method [25]. Figure 2 shows the zonal flow amplitude coefficients U_p as functions of q at $\mu = 0.21$ and $\mu = 0.19$. Near the instability threshold, ideal states exist at all q for which the homogeneous equilibrium is zonostrophically unstable [between the two lines labeled N in Fig. 2(a)]. Farther from threshold, there is a region of q where the ideal state solution disappears [between the lines N and D in Fig. 2(b); see also Fig. 3]. The values of the other parameters used are $\beta = 1$, $\nu = 10^{-3}$, and $h = 4$. The forcing F acts equally on wave vectors \mathbf{k} with $7/8 < |\mathbf{k}| < 9/8$. The forcing provides a total energy input of $\varepsilon = 1$.

Stability of the Ideal States To investigate stability of the ideal states, we consider perturbations $\delta W(x, y | \bar{y}, t)$ and $\delta U(\bar{y}, t)$ about an equilibrium W, U . The linearized

CE2 equations are

$$\begin{aligned} \partial_t \delta W = & -(\delta U_1 - \delta U_2) \partial_x W - (U_1 - U_2) \partial_x \delta W \\ & + (\delta U_1'' - \delta U_2'') (\nabla^2 + \frac{1}{4} \partial_{\bar{y}}^2) \partial_x C \\ & + (U_1'' + U_2'') (\nabla^2 + \frac{1}{4} \partial_{\bar{y}}^2) \partial_x \delta C \\ & - (\delta U_1'' + \delta U_2'') \partial_{\bar{y}} \partial_y \partial_x C - (U_1'' + U_2'') \partial_{\bar{y}} \partial_y \partial_x \delta C \\ & + 2\beta \partial_{\bar{y}} \partial_y \partial_x \delta C - 2(\mu + \nu D_h) \delta W, \end{aligned} \quad (7a)$$

$$\partial_t \delta U = -[\mu + \nu(-1)^h \partial_{\bar{y}}^{2h}] \delta U - \partial_{\bar{y}} \partial_y \partial_x \delta C(0, 0 | \bar{y}, t). \quad (7b)$$

Since the underlying equilibrium is periodic in \bar{y} , the perturbations can be expanded as a Bloch state [16, 19]:

$$\delta W(x, y | \bar{y}, t) = e^{\sigma t} e^{iQ\bar{y}} \sum_{mnp} \delta W_{mnp} e^{imax} e^{inby} e^{ipq\bar{y}}, \quad (8a)$$

$$\delta U(\bar{y}, t) = e^{\sigma t} e^{iQ\bar{y}} \sum_p \delta U_p e^{ipq\bar{y}}, \quad (8b)$$

where Q is the Bloch wave number and can be taken to lie within the first Brillouin zone $-q/2 < Q \leq q/2$. We do not use a Q_x or Q_y because as previously mentioned the periodicity in x and y is artificial. Equation (7) is projected onto the basis functions in the same way as in the ideal state calculation. This projection results in a linear system at each Q for the coefficients δW_{mnp} and δU_p ; this determines an eigenvalue problem for σ . The equilibrium is unstable if for any Q there are any eigenvalues with $\text{Re } \sigma > 0$.

The stable ideal states exist within the closed region, known as the stability balloon, shown in Fig. 3. We adopt the friction μ as the control parameter, but plot using $-\mu$ because stability balloons are conventionally depicted with destabilization parameters. The stability balloon is bounded by curves representing marginal stability due to various instabilities. These curves are determined near threshold ($\mu = \mu_c = 0.24$) by the Eckhaus instability, a long-wavelength universal instability, and farther from threshold by various short-wavelength instabilities. Details of these instabilities will be reported in a subsequent article.

For $0.07 < \mu < \mu_c$, the stability balloon is consistent with the QL zonal flow wave numbers obtained in [11]. On the other hand, for $\mu < 0.07$ there is some discrepancy between CE2 and the QL system. CE2 predicts no steady states, and indeed, numerical simulations of the CE2 equations display translating zonal jets. In contrast, the QL system exhibits seemingly steady zonal jets for even for these small values of μ [11]. This discrepancy warrants further investigation.

Discussion Numerical simulations typically occur within a finite domain. When periodic boundary conditions are used, our infinite-domain results are modified merely by the discretization of wave numbers. This affects not only the possible equilibria, but also any perturbations and hence the stability boundaries too.

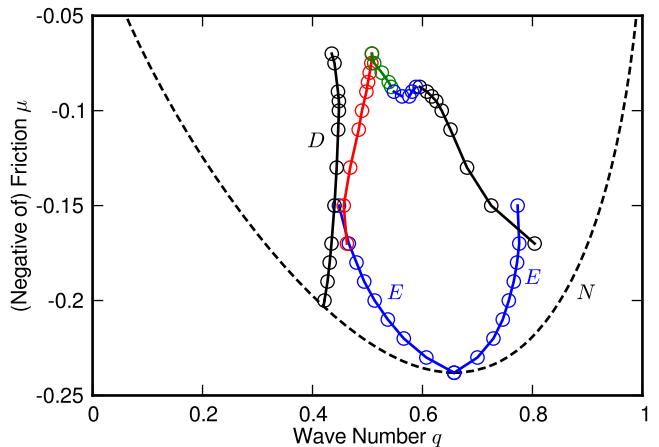


FIG. 3. Stability balloon for the CE2 equations. Above the neutral curve (N), the homogeneous turbulent state is zonotrophically unstable. Ideal states are stable within the closed region. The solution branch of stationary ideal states vanishes to the left of D. Near threshold the stability balloon is determined by the Eckhaus instability (E).

For a time-evolving system, the exact q that is ultimately chosen within the stability balloon results from a dynamical process and is not addressed in a systematic way by the present study.

While the CE2 equations exhibit spontaneously generated zonal flows, it is true that they neglect many physical effects. An important piece of physics missing from the CE2 equations is the nonlinear eddy self-interaction, which clearly cannot be ignored in general. Furthermore, the CE2 equations involve one-time correlation functions rather than the more general two-time functions. The lack of time-history information means that most of the effects of wave propagation are discarded [26]. At least one particular instance of the qualitative failure of CE2 has been noted [27].

Yet, the basic mathematical structure of the theory presented here arises only from symmetry arguments and general properties of the zonotrophic instability. If one were to include the important physics neglected in CE2, those general symmetries and properties should remain intact. Therefore, we expect our qualitative conclusions to likewise remain valid.

In summary, by analyzing a second-order statistical model of an ensemble of interacting zonal flows and turbulence, we have shown that zonal flows constitute pattern formation amid a turbulent bath. We calculated the stability balloon of steady zonal jets and explained the merging of jets as a means of attaining a stable wave number. In general, the use of statistically averaged equations and the pattern formation methodology provides a path forward for further systematic investigations of zonal flows and their interactions with turbulence.

We acknowledge useful discussions with Brian Farrell, Henry Greenside, Petros Ioannou, and Brad Marston.

This material is based upon work supported by an NSF Graduate Research Fellowship and a US DOE Fusion Energy Sciences Fellowship. This work was also supported by US DOE Contract DE-AC02-09CH11466.

* jbparker@princeton.edu

† krommes@princeton.edu

- [1] A. R. Vasavada and A. P. Showman, Rep. Prog. Phys. **68**, 1935 (2005).
- [2] N. A. Maximenko, B. Bang, and H. Sasaki, Geophys. Res. Lett. **32**, L12607 (2005).
- [3] A. Fujisawa, Nucl. Fusion **49**, 013001 (2009).
- [4] A. Johansen, A. Youdin, and H. Klahr, Astrophys. J. **697**, 1269 (2009).
- [5] Z. Lin, T. S. Hahm, W. W. Lee, W. M. Tang, and R. B. White, Science **281**, 1835 (1998).
- [6] P. B. Rhines, J. Fluid Mech. **69**, 417 (1975).
- [7] G. K. Vallis and M. E. Maltrud, J. Phys. Oceanogr. **23**, 1346 (1993).
- [8] S. Sukoriansky, N. Dikovskaya, and B. Galperin, J. Atmos. Sci. **64**, 3312 (2007).
- [9] H.-P. Huang and W. A. Robinson, J. Atmos. Sci. **55**, 611 (1998).
- [10] R. K. Scott and L. M. Polvani, J. Atmos. Sci. **64**, 3158 (2007).
- [11] K. Srinivasan and W. R. Young, J. Atmos. Sci. **69**, 1633 (2012).
- [12] A. I. Smolyakov, P. H. Diamond, and M. Malkov, Phys. Rev. Lett. **84**, 491 (2000).
- [13] J. A. Krommes and C.-B. Kim, Phys. Rev. E **62**, 8508 (2000).
- [14] J. A. Krommes, Physics Reports **360**, 1 (2002).
- [15] M. C. Cross and P. C. Hohenberg, Rev. Mod. Phys. **65**, 851 (1993).
- [16] M. Cross and H. Greenside, *Pattern Formation and Dynamics in Nonequilibrium Systems* (Cambridge University Press, 2009).
- [17] R. Hoyle, *Pattern Formation: An Introduction to Methods* (Cambridge University Press, 2006).
- [18] F. H. Busse, Rep. Prog. Phys. **41**, 1929 (1978).
- [19] R. M. Clever and F. H. Busse, J. Fluid Mech. **65**, 625 (1974).
- [20] A. C. Newell, T. Passot, and M. Souli, J. Fluid Mech. **220**, 187 (1990).
- [21] B. F. Farrell and P. J. Ioannou, J. Atmos. Sci. **60**, 2101 (2003).
- [22] B. F. Farrell and P. J. Ioannou, J. Atmos. Sci. **64**, 3652 (2007).
- [23] J. B. Marston, E. Conover, and T. Schneider, J. Atmos. Sci. **65**, 1955 (2008).
- [24] S. M. Tobias, K. Dagon, and J. B. Marston, Astrophys. J. **727**, 127 (2011).
- [25] C. T. Kelley, *Solving Nonlinear Equations with Newton's Method* (Society for Industrial and Applied Mathematics, 2003).
- [26] J. A. Krommes and R. A. Smith, Ann. Phys. **177**, 246 (1987).
- [27] S. M. Tobias and J. B. Marston, "Direct statistical simulation of out-of-equilibrium jets," (2012), arXiv:physics.flu-dyn/1209.3862v1.